BIOCHEMISTRY
including biophysical chemistry & molecular biology

Article

pubs.acs.org/biochemistry

# Characterizing the Importance of the Biotin Carboxylase Domain Dimer for *Staphylococcus aureus* Pyruvate Carboxylase Catalysis

Linda P. C. Yu,[†] Chi-Yuan Chou,[‡] Philip H. Choi,[†] and Liang Tong*[,†]

[†]Department of Biological Sciences, Columbia University, New York, New York 10027, United States

[‡]Department of Life Sciences and Institute of Genome Sciences, National Yang-Ming University, Taipei 112, Taiwan

**ABSTRACT:** Biotin carboxylase (BC) is a conserved component among biotin-dependent carboxylases and catalyzes the MgATP-dependent carboxylation of biotin, using bicarbonate as the $CO_2$ donor. Studies with *Escherichia coli* BC have suggested long-range communication between the two active sites of a dimer, although its mechanism is not well understood. In addition, mutations in the dimer interface can produce stable monomers that are still catalytically active. A homologous dimer for the BC domain is observed in the structure of the tetrameric pyruvate carboxylase (PC) holoenzyme. We have introduced site-specific mutations into the BC domain dimer interface of *Staphylococcus aureus* PC (SaPC), equivalent to those used for *E. coli* BC, and also made chimeras replacing the SaPC BC domain with the *E. coli* BC subunit (EcBC chimera) or the yeast ACC BC domain (ScBC chimera). We assessed the catalytic activities of these mutants and characterized their oligomerization states by gel filtration and analytical ultracentrifugation experiments. The K442E mutant and the ScBC chimera disrupted the BC dimer and were catalytically inactive, while the F403A mutant and the EcBC chimera were still tetrameric and retained catalytic activity. The R54E mutant was also tetrameric but was catalytically inactive. Crystal structures of the R54E, F403A, and K442E mutants showed that they were tetrameric in the crystal, with conformational changes near the mutation site as well as in the tetramer organization. We have also produced the isolated BC domain of SaPC. In contrast to *E. coli* BC, the SaPC BC domain is monomeric in solution and catalytically inactive.

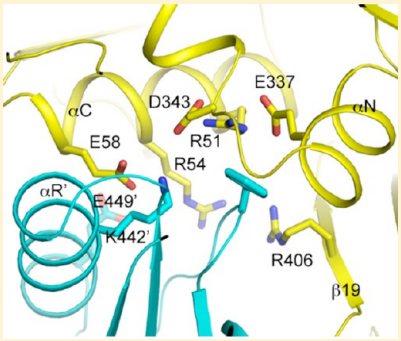


Biotin-dependent carboxylases are widely distributed in nature and have important functions in many metabolic processes.[1−5] They carry two distinct catalytic activities.[6] A biotin carboxylase (BC) activity catalyzes the $Mg^{2+}$-ATP-dependent carboxylation of biotin, using bicarbonate as the $CO_2$ donor. Then a carboxyltransferase (CT) activity transfers the carboxyl group from carboxybiotin to the acceptor, which oftentimes is the coenzyme A (CoA) ester of an organic acid (acetyl-CoA, propionyl-CoA, etc.) but can also be a small compound (pyruvate or urea). Biotin is covalently linked to a biotin carboxyl carrier protein (BCCP) component.

The BC activity is common among these enzymes, and the amino acid sequences of this component are well conserved among them. The BC subunit of *Escherichia coli* acetyl-CoA carboxylase (ACC) has been used as a model system to study this activity.[7−10] It can catalyze the carboxylation of free biotin, in the absence of the CT and BCCP subunits of the ACC holoenzyme. The crystal structures of its free enzyme,[11] the ATP complex,[12,13] and the pentanary complex with Mg-ADP, biotin, and bicarbonate[14] are all available. The BC structure contains three domains, named A−C, and the active site is located at the interface among them (Figure 1A). Domain B undergoes a large rearrangement and closes over the active site during catalysis.[12,14]

The *E. coli* BC subunit is a stable dimer, formed by interaction among the A and C domains of the two monomers (Figure 1A). The active site of each monomer is ∼25 Å from the dimer interface, with no contribution from residues in the other monomer. However, mutagenesis studies showed that knocking out the active site of one monomer of the dimer essentially abolished catalysis at the other active site, suggesting long-range communications between the two active sites and the importance of dimerization for BC catalysis.[15] An asymmetric structure of *E. coli* BC with only one of the two active sites occupied by an ATP analogue ($ADPCF_2P$) has been observed,[13] and mathematical simulations also support this half-sites reactivity.[16] In addition, the BC domain of eukaryotic ACC is monomeric in solution and is catalytically inactive,[17,18] in apparent agreement with this model.

On the other hand, mutations in the dimer interface of *E. coli* BC can generate stable monomers of the enzyme, and these monomeric mutants can still catalyze the BC reaction.[19,20] Moreover, the BC domain is monomeric in the $\alpha_6\beta_6$ holoenzyme of propionyl-CoA carboxylase,[21] shows trimeric association in the $\alpha_6\beta_6$ holoenzyme of 3-methylcrotonyl-CoA carboxylase,[22] and is monomeric in urea carboxylase.[23] Therefore, dimerization, per se, may not be required for the catalytic activity of BC. The mechanism for long-range communication between the two active sites in the *E. coli* BC dimer is still not fully understood.

**Received:** September 22, 2012
**Revised:** December 10, 2012
**Published:** January 3, 2013

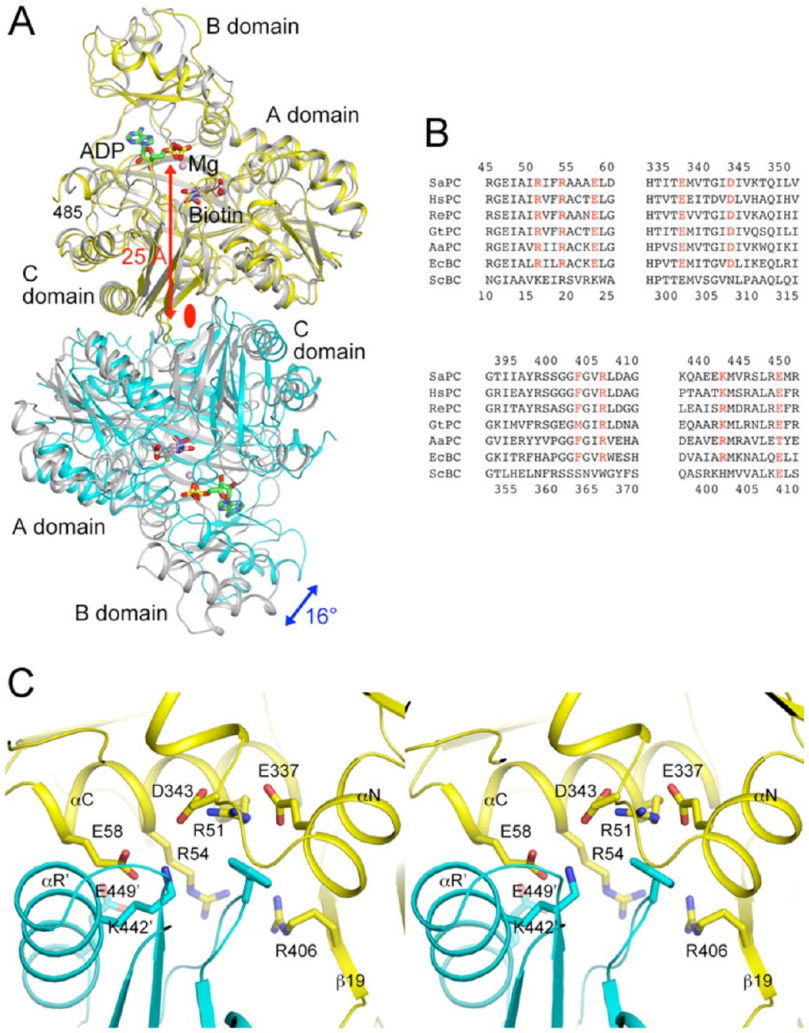


**Figure 1.** Conserved BC domain dimer interface for SaPC and *E. coli* BC. (A) Overlay of the structures of the BC domain dimer of the SaPC free enzyme (yellow and cyan for the two monomers)[25] and the *E. coli* BC dimer (gray) in complex with ADP (green), $Mg^{2+}$ (pink sphere), bicarbonate (black), and biotin (pink).[14] The blue arrow indicates the difference in orientation for the second monomer of the dimer between the two structures, and the red arrow indicates the distance from the dimer interface to the active site. The two-fold axis of the dimer is indicated with the red oval. (B) Alignment of amino acid sequences in the dimer interface region for SaPC, human PC (HsPC), RePC, *Geobacillus thermodenitrificans* PC (GtPC), *Aquifex aeolicus* PC (AaPC), *E. coli* BC (EcBC), and the BC domain of yeast ACC (ScBC). Residues having important interactions in the interface are colored red. Residue numbers at the top are for SaPC (in human PC numbering), and those at the bottom are for *E. coli* BC. (C) Detailed interactions at the BC domain dimer interface of SaPC. Residues Arg54, Glu58, Phe403, and Lys442 were selected for mutagenesis. The primed residue numbers indicate the second monomer. All structural figures were produced with PyMOL (http://www.pymol.org).

The BC domain dimer in the structures of the tetrameric holoenzyme of pyruvate carboxylase (PC)[24−27] has an organization similar to that of the BC subunit dimer of *E. coli* ACC (Figure 1A). Residues in the dimer interface of the two enzymes are generally conserved (Figure 1B) and show similar interactions (Figure 1C). To further study the importance of the BC dimer interface for catalysis, we have introduced mutations of this interface into full-length *Staphylococcus aureus* PC (SaPC) as well as its isolated BC domain. The mutations are equivalent to those that destabilized the dimer of *E. coli* BC[19] and include R54E, E58R, F403A, and K442E. In addition, we have created chimeric PCs, replacing its BC domain with the BC subunit of *E. coli* ACC (EcBC chimera) or the BC domain of yeast ACC (ScBC chimera). Our studies showed that the K442E mutant and the ScBC chimera have disrupted the tetramer of PC in solution and are catalytically inactive.

## MATERIALS AND METHODS

**Mutagenesis, Protein Expression, and Purification.** The dimer interface mutants of full-length SaPC were made using the QuikChange kit (Stratagene) and sequenced to verify successful mutagenesis. The mutants were overexpressed in *E. coli* BL21(DE3) Star cells at 20 °C and purified by Ni-NTA and Sephacryl-S300 (GE Healthcare) gel filtration chromatography. The expression construct introduced an N-terminal hexahistidine tag into the protein. The purified protein was concentrated to 20 mg/mL and flash-frozen with liquid nitrogen in a buffer containing 20 mM Tris (pH 7.5), 200 mM NaCl, 2 mM dithiothreitol (DTT), and 5% (v/v) glycerol.

The EcBC and ScBC chimeras were designed on the basis of the overlay of the structures of *E. coli* and *Saccharomyces cerevisiae* BC with the BC domain of SaPC. A residue close to the C-terminus of the *E. coli* or *S. cerevisiae* BC, located in a hydrophilic segment on the surface, and structurally similar to


dx.doi.org/10.1021/bi301294d | *Biochemistry* 2013, 52, 488−496

SaPC, was chosen as the connection point for the chimera. The chimera constructs were made by overlapping polymerase chain reaction.

The isolated BC domain of SaPC was created by introducing a STOP codon after amino acid 455 (486 in human PC numbering) through mutagenesis. Mutations in the dimer interface were then introduced, equivalent to those for full-length SaPC. These BC proteins were expressed and purified following the same protocol that was used for the full-length protein.

**Analytical Ultracentrifugation (AUC).** The sedimentation velocity (SV) experiments were performed using an XL-A analytical ultracentrifuge with a standard 12 mm double-sector *Epon* charcoal-filled centerpiece (Beckman, Fullerton, CA). The sample (330 $\mu$L) and reference (370 $\mu$L) solutions were loaded into the centerpiece and mounted in an An-50 Ti rotor. The experiments were performed at 20 °C with a rotor speed of 42000 rpm. The absorbance at 280 nm was chosen to detect the protein, which was monitored in a continuous mode with a time interval of 480 s and a step size of 0.003 cm. Three different protein concentrations (0.4−10 $\mu$M) were used to estimate the dynamic monomer−dimer or monomer−dimer−tetramer association. The SV results at three protein concentrations were then globally analyzed using a monomer−dimer or monomer−dimer−tetramer equilibrium model with SEDPHAT.[28]

To characterize the size distributions of the various proteins in solution, the scans at different time intervals were fit to a continuous $c(s)$ distribution model using SEDFIT.[29,30] The size distributions for sedimentation coefficients between 0 and 20 S are solved and regularized at a confidence level of $p = 0.95$ by maximal entropy.

**Enzyme Assays.** The catalytic activity of full-length wild-type and mutant SaPC was determined spectrophotometrically at 340 nm, following a published protocol that couples the production of oxaloacetate to the oxidation of NADH.[31] Pyruvate titrations (up to 40 mM) were performed in the absence of acetyl-CoA. The effect of acetyl-CoA on SaPC activity was assayed at 5 mM pyruvate, which is the $K_m$ for this substrate for wild-type SaPC.

The catalytic activity of the BC domain of SaPC was determined following an established ATP hydrolysis assay,[9] which couples ADP production to NADH oxidation. The reaction mixture (0.2 mL) contained 100 mM Hepes (pH 8.5), 8 mM $MgCl_2$, 40 mM biotin, 200 mM NaCl, 50 mM $Na_2CO_3$, 0.2 mM NADH, 0.5 mM phosphoenolpyruvate, 20 units/mL lactate dehydrogenase/pyruvate kinase, 400 nM SaPC BC domain (in terms of the monomer), and varying concentrations of ATP, which was added last to the reaction mixture.

**Protein Crystallization.** Full-length SaPC carrying the R54E, F403A, or K442E mutation was crystallized under the same conditions as wild-type SaPC.[25] The protein, at 10 mg/mL, was incubated with 5 mM ATP at 4 °C for 1 h and then mixed in a 1:1 ratio with a reservoir solution that contained 200 mM ammonium tartrate and 20% (w/v) PEG 3350. Crystals were grown using the sitting-drop vapor diffusion method at 21 °C, cryoprotected with a solution consisting of the reservoir solution supplemented with 20% (v/v) ethylene glycol, and flash-frozen in liquid nitrogen for the collection of data at 100 K.

Extensive efforts to crystallize the BC domain of SaPC (wild type and mutants) were unsuccessful.

**Data Collection, Structure Determination, and Refinement.** X-ray diffraction data were collected at the X29A beamline of the National Synchrotron Light Source (NSLS). The diffraction images were processed and scaled with the HKL package.[32] The mutant crystals have unit cell parameters similar to those of wild-type SaPC,[25] and there is one tetramer in the asymmetric unit. The structures were determined by the molecular replacement method with COMO,[33] using the structure of wild-type SaPC as the search model.[25] Structure refinement was conducted with CNS[34] and Refmac,[35] and manual rebuilding of the atomic models was performed with O[36] and Coot.[37] The data processing and refinement statistics are summarized in Table 1. The difference between $R$ and $R_{free}$ is ∼7% for the three structures, indicating possibly some overfitting in the model.

**Table 1. Summary of Crystallographic Information**[a]

| | R54E | F403A | K442E |
|---|---|---|---|
| | Data Collection | | |
| space group | $P2_1$ | $P2_1$ | $P2_1$ |
| cell dimensions | | | |
| *a*, *b*, *c* (Å) | 96.4, 256.7, 127.0 | 96.2, 256.3, 126.7 | 96.6, 258.5, 126.9 |
| $\alpha$, $\beta$, $\gamma$ (deg) | 90, 109.3, 90 | 90, 109.8, 90 | 90, 109.6, 90 |
| resolution range (Å) | 30−2.8 (2.9−2.8) | 30−2.8 (2.9−2.8) | 30−3.0 (3.1−3.0) |
| $R_{merge}$ (%) | 12.5 (44.7) | 9.2 (46.5) | 6.5 (42.9) |
| $I/\sigma I$ | 10.5 (3.5) | 11.7 (2.1) | 15.5 (2.5) |
| completeness (%) | 93 (86) | 91 (94) | 98 (99) |
| redundancy | 4.7 (4.8) | 2.8 (2.8) | 2.8 (2.7) |
| | Refinement | | |
| no. of reflections | 125986 | 122029 | 109041 |
| $R$ (%) | 19.4 (26.6) | 20.9 (25.7) | 19.4 (24.5) |
| $R_{free}$ (%) | 26.2 (35.2) | 27.9 (35.3) | 26.2 (33.1) |
| no. of atoms | | | |
| protein | 34009 | 32422 | 32401 |
| ligand | 63 | 62 | 31 |
| water | 0 | 0 | 0 |
| average *B* value (Å$^2$) | | | |
| protein | 26.2 | 49.0 | 40.2 |
| ligand | 81.6 | 101.1 | 118.8 |
| root-mean-square deviation | | | |
| bond lengths (Å) | 0.011 | 0.013 | 0.011 |
| bond angles (deg) | 1.3 | 1.4 | 1.2 |

[a]The numbers in parentheses are for the highest-resolution shell.

## RESULTS AND DISCUSSION

**Design of Mutations in the BC Dimer Interface of SaPC.** The BC domain dimer of SaPC has an overall organization similar to that of the *E. coli* BC dimer (Figure 1A). With one monomer of the two dimers in superposition, the orientation of the other monomer differs by a 16° rotation. Residues that have interactions in the *E. coli* BC dimer interface are generally conserved in SaPC (Figure 1B) and show similar interactions in its BC dimer interface, as well (Figure 1C). For example, Arg54 and Glu58 [equivalent to Arg19 and Glu23 of *E. coli* BC, respectively (Figure 1B)] have ion pair interactions with Glu4492 and Lys4422 (Glu4082 and Arg4012 in *E. coli* BC), respectively (with the primed residue numbers indicating the other monomer) (Figure 1C). Residues in SaPC are numbered

according to their equivalents in human PC unless noted otherwise.[25] Arg51 (Arg16 in *E. coli* BC) has ion pair interactions with Glu337 and Asp343, which are in the binding site for Phe4032 (Phe3632 in *E. coli* BC).

Previous studies with *E. coli* BC showed that the R16E, R19E, and E23R mutations greatly destabilized the BC dimer, giving rise to 5000−8000-fold increases in the $K_d$, while the F363A mutation led to an only 4-fold increase in the $K_d$ of the dimer.[19,20] The R401E mutant of *E. coli* BC was also produced, but the resulting protein was mostly aggregated.[19]

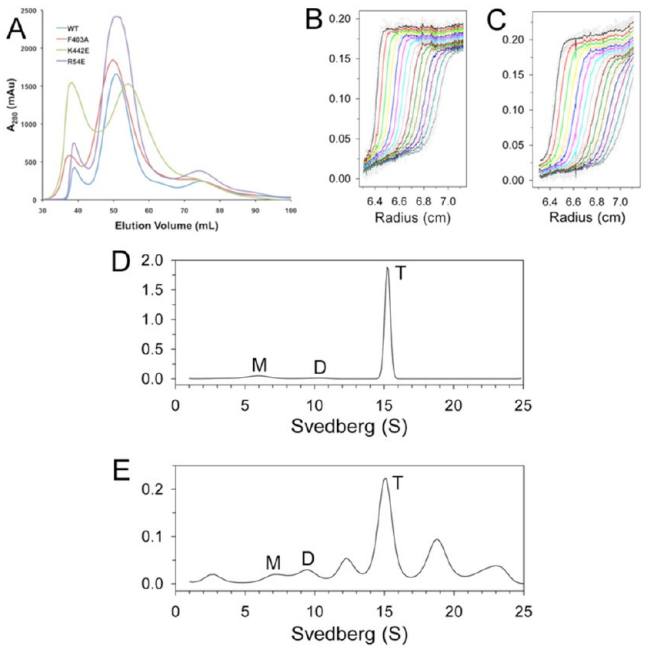


**Figure 2.** Oligomerization states of the dimer interface mutants in solution. (A) Gel filtration profiles (from an S300 column) for wild-type SaPC and the dimer interface mutants. (B) Sedimentation velocity AUC data for wild-type SaPC at a concentration of 1.5 $\mu$M. The observed data are shown as empty circles, and the theoretical fit to the data based on a rapid monomer−dimer−tetramer association model is shown as the curves. (C) Sedimentation velocity AUC data for the K442E mutant at a concentration of 1.5 $\mu$M. (D) Size distributions of wild-type SaPC in solution at a concentration of 1 mg/mL, based on the best-fit results by the continuous size distribution analysis:[30] M, monomer; D, dimer; T, tetramer. (E) Size distributions of the EcBC chimera in solution at a concentration of 1 mg/mL.

To study the effects of the BC dimer interface on SaPC catalysis, we created four single-site mutants in this interface, R54E, E58R, F403A, and K442E, which are equivalent to the R19E, E23R, F363A, and R401E mutants, respectively, in the *E. coli* dimer interface that we studied previously.[19] In addition, we created two chimeric PC proteins, replacing the BC domain of SaPC (residues 1−448 in SaPC numbering and 34−481 in human PC numbering) with the BC subunit of *E. coli* BC (residues 1−440) or the BC domain (residues 1−562) of yeast ACC.[17] We expect that the chimera with the *E. coli* BC (to be termed the EcBC chimera) may be able to maintain the tetrameric organization of wild-type SaPC and might be catalytically active, as well. In contrast, the chimera with the yeast BC domain (to be termed the ScBC chimera) may no longer be tetrameric, as the yeast BC domain itself is monomeric.[17] Many of the residues in the dimer interface of *E. coli* BC are not conserved in yeast BC (Figure 1B). More importantly, yeast BC has a different structure in this region, which is incompatible with the mode of dimerization for *E. coli* BC.[17]

**Mutations in the BC Dimer Interface Can Disrupt the SaPC Tetramer.** Wild-type SaPC and the various mutants were overexpressed in *E. coli* and purified by nickel affinity and gel filtration chromatography. The gel filtration profiles show that wild-type SaPC, the R54E and F403A single-site mutants, and the EcBC chimera migrated at the same position, indicating that they are tetrameric during purification (Figure 2A). In contrast, the K442E mutant and the ScBC chimera migrated slower on the gel filtration column, suggesting that they may have become dimeric. Finally, the E58R mutant produced aggregated proteins, and this mutant was not studied further.

We next conducted analytical ultracentrifugation (AUC) experiments to study in more detail the oligomerization behavior of these proteins. Sedimentation velocity data were fit to a rapid monomer−dimer−tetramer association model, from which the $K_d$ values for monomer−dimer and dimer−tetramer association were determined. Wild-type SaPC has a $K_d$ of 0.75 $\mu$M for the monomer−dimer equilibrium and 8 nM for the dimer−tetramer association (Figure 2B and Table 2). The R54E and F403A mutants behaved essentially the same as the wild-type enzyme in these experiments. In contrast, the K442E

**Table 2. Summary of Analytical Ultracentrifugation and Kinetic Data**

| protein | $K_d$ ($\mu$M)[b] (monomer−dimer) | $K_d$ ($\mu$M)[b] (dimer−tetramer) | $k_{cat}$ ($s^{-1}$) | $K_m$ (mM) (for pyruvate) | $k_{cat}/K_m$ ($s^{-1}$ $M^{-1}$) |
|---|---|---|---|---|---|
| | | Full-Length SaPC[a] | | | |
| wild-type | 0.75 ± 0.06 | 0.008 ± 0.0006 | 20.2 ± 1.4 | 3.4 ± 0.8 | 5900 ± 1400 |
| R54E | 0.53 ± 0.03 | 0.003 ± 0.0001 | NA[c] | NA[c] | NA[c] |
| F403A | 0.45 ± 0.04 | 0.011 ± 0.0006 | 1.3 ± 0.1 | 1.4 ± 0.4 | 930 ± 270 |
| K442E | 0.82 ± 0.09 | 840 ± 190 | NA[c] | NA[c] | NA[c] |
| EcBC chimera | 2.31 ± 0.33 | 0.28 ± 0.03 | 1.1 ± 0.1 | 0.34 ± 0.02 | 3300 ± 200 |
| ScBC chimera | 0.56 ± 0.06 | 68 ± 11 | NA[c] | NA[c] | NA[c] |
| | | BC Domain of SaPC[a] | | | |
| wild-type | 48 ± 4 | – | NA[c] | NA[c] | NA[c] |
| R54E | 195 ± 7 | – | NA[c] | NA[c] | NA[c] |
| F403A | 130 ± 6 | – | NA[c] | NA[c] | NA[c] |
| K442E | 86 ± 8 | – | NA[c] | NA[c] | NA[c] |

[a]The protein concentrations for full-length SaPC were 0.4, 1.5, and 7.4 $\mu$M (based on monomer) in the AUC experiment, and those for the BC domain were 1, 4, and 10 $\mu$M. [b]For full-length SaPC, the $K_d$ values were the best-fit results based on a rapid monomer−dimer−tetramer association model, and the local root-mean-square deviation (rmsd) was from 0.0041 to 0.0210. For the BC domain alone, a rapid monomer−dimer association model was used, and the local rmsd was from 0.0037 to 0.0070. [c]No activity was observed under the condition tested.


dx.doi.org/10.1021/bi301294d | *Biochemistry* 2013, 52, 488−496

mutant had a $K_d$ of 840 $\mu$M for the dimer−tetramer association (Figure 2C), consistent with the gel filtration data and confirming that this mutation has disrupted the tetramer of SaPC. The AUC data also showed that the EcBC chimera formed a tetramer in solution, although the $K_d$ for the dimer−tetramer association was ∼35-fold higher than that of wild-type SaPC. The ScBC chimera is dimeric in solution, consistent with our expectations and the gel filtration data.

**Table 3. Size Distributions of SaPC in Solution**

| protein[a] | monomer (%) | dimer (%) | tetramer (%) | other (%) |
|---|---|---|---|---|
| Full-Length SaPC | | | | |
| wild-type | 11 | 2 | 85 | <5 |
| R54E | 4 | 0 | 96 | <5 |
| F403A | 9 | 2 | 85 | <5 |
| K442E | 10 | 65 | – | ∼25 |
| EcBC chimera | 5 | 7 | 34 | ∼55 |
| ScBC chimera | 22 | 71 | – | <10 |
| BC Domain of SaPC | | | | |
| wild-type | 37 | 20 | – | ∼40 |
| R54E | 86 | 9 | – | ∼5 |
| F403A | 67 | 12 | – | ∼20 |
| K442E | 41 | 14 | – | ∼45 |

[a]The distribution was observed by AUC. The protein concentration was 1 mg/mL (∼7.5 $\mu$M for full-length SaPC and ∼20 $\mu$M for the isolated BC domain, based on the monomer).

The $K_d$ values for monomer−dimer association of the two mutants that were dimeric in solution, K442E and the ScBC chimera, were essentially the same as that of wild-type SaPC (Table 2). The SaPC tetramer is formed by interactions at the BC, CT, and PT (PC tetramerization domain) dimer interfaces.[25] The AUC data for these mutants suggest that the CT and PT domains may be sufficient to mediate their dimerization.

To further characterize the oligomerization behavior of these proteins, we used AUC sedimentation velocity experiments to examine their size distributions in solution at a concentration of 1 mg/mL. Wild-type SaPC (Figure 2D) and the R54E and F403A mutants were predominantly tetrameric, with roughly 10% of the species being monomeric under the experimental condition tested (Table 3). In contrast, the K442E mutant and the ScBC chimera were mostly dimeric in solution, with the K442E mutant also showing signs of aggregation (Table 3). Somewhat surprisingly, while the EcBC chimera was able to form tetramers in solution, it also showed a significant amount of aggregation (Figure 2E and Table 3).

**Mutations in the BC Dimer Interface Can Disrupt SaPC Catalysis.** We next characterized the catalytic activity of the various proteins, using a coupled enzyme assay that converted the oxaloacetate product of pyruvate carboxylation to NADH oxidation.[31] Good catalytic activity was observed for the wild-type enzyme (Table 2). Among the dimer interface mutants, only the F403A mutant exhibited catalytic activity,

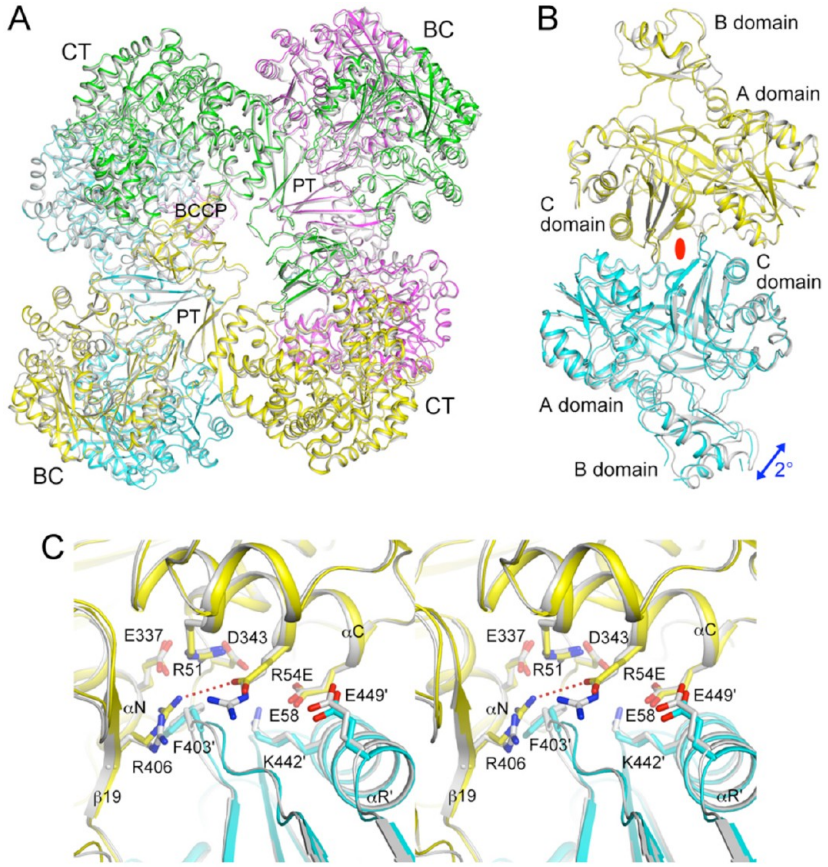


**Figure 3.** R54E mutant that has only small structural differences vs wild-type SaPC. (A) Overlay of the structures of the R54E mutant tetramer (in color for the four monomers, yellow, magenta, cyan, and green) and wild-type SaPC (gray). The superposition is based on the BC domain of the first monomer (yellow). (B) Overlay of the structures of the R54E mutant BC domain dimer (yellow and cyan) and wild-type SaPC dimer (gray). The blue arrow indicates the difference in orientation for the second monomer of the dimer between the two structures. The two-fold axis of the dimer is indicated with the red oval. (C) Close-up of the BC domain dimer interface near the mutation site.


dx.doi.org/10.1021/bi301294d | *Biochemistry* 2013, 52, 488−496

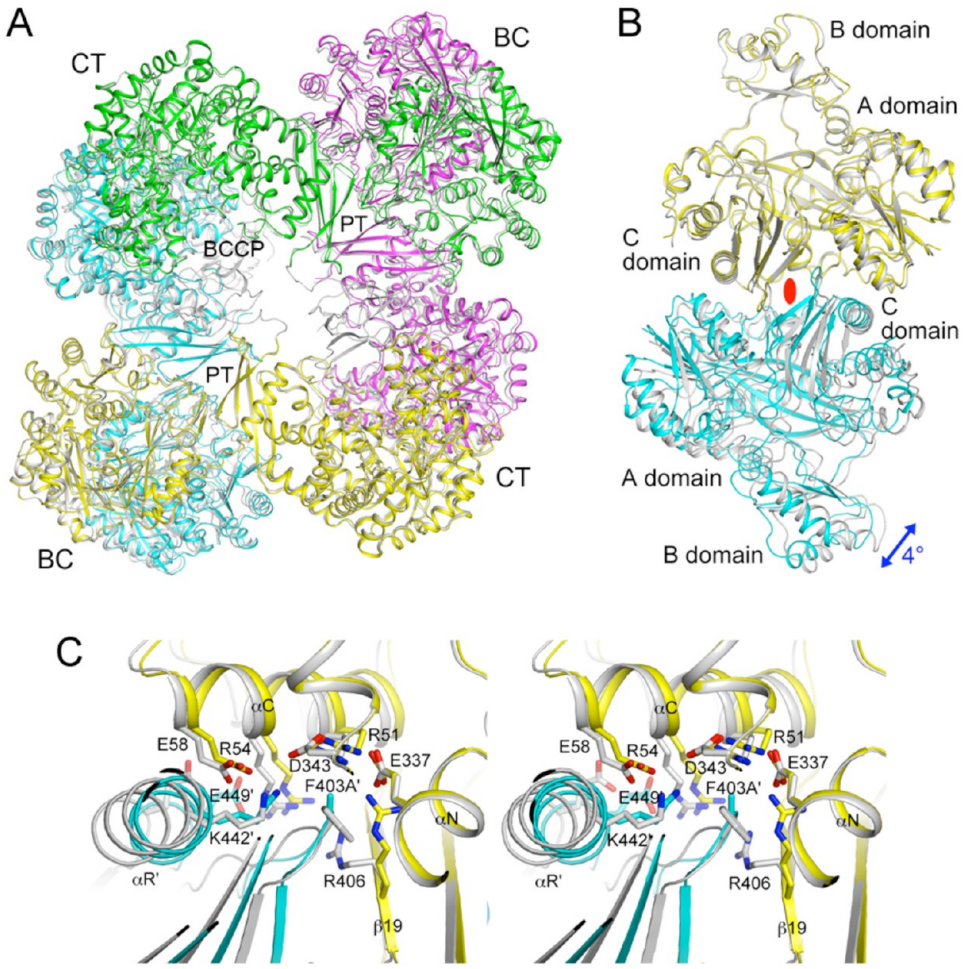


**Figure 4.** F403A mutant that shows large structural differences vs wild-type SaPC. (A) Overlay of the structures of the F403A mutant tetramer (in color) and wild-type SaPC (gray). The superposition is based on the BC domain of the first monomer (yellow). (B) Overlay of the structures of the F403A mutant BC domain dimer (yellow and cyan) and wild-type SaPC dimer (gray). (C) Close-up of the BC domain dimer interface near the mutation site.

with ~6-fold lower $k_{cat}/K_m$ than the wild-type enzyme. The concentration of the enzyme in these assays was ~0.1 $\mu$M (based on the monomer), and therefore, the observed lack of activity for the K442E mutant and the ScBC chimera is consistent with the AUC data. These proteins are dimeric in solution at this concentration, but PC is only active in the tetrameric form. On the other hand, it is not clear why the R54E mutant is inactive, as it is a tetramer in solution. The EcBC chimera had ~2-fold lower $k_{cat}/K_m$ than the wild-type enzyme, although its $k_{cat}$ is ~20-fold lower (Table 2). We also tested the intrinsic ATPase activity of the ScBC chimera and found very weak (if any) activity.

Wild-type SaPC, like most other PCs, is activated by acetyl-CoA. This compound binds at the interface between two BC domains of the tetramer,[24,26] and it can also rescue the catalytic activity of a mutant carrying a change in the PT dimer interface of SaPC.[25] In contrast, acetyl-CoA had no effect on the catalytic activity of the BC dimer interface mutants and the chimeras studied here.

**The Dimer Interface Mutants Are Still Tetrameric in the Crystal.** To characterize the effects of mutations in the BC domain dimer interface on the structure of SaPC, we next determined the crystal structures of the R54E, F403A, and K442E mutants at up to 2.8 Å resolution (Table 1). The mutants crystallized under the same condition as wild-type SaPC. The crystal structures have been deposited in the Protein Data Bank (entries 4HNT, 4HNU, and 4HNV). The R54E and F403A mutants existed as tetramers in the crystal, as the mutations did not affect the $K_d$ (Table 3). Surprisingly, the K442E mutant was also found to be tetrameric in the crystal, even though the $K_d$ for its tetramer is 840 $\mu$M (Table 2). The high concentration of the protein in the crystalline environment (~50 $\mu$M in the crystallization solution and ~4.5 mM in the crystal) and the presence of the ATP substrate may have promoted the formation of the tetramer. It is also possible that the crystal stabilized and selectively sequestered the tetrameric form of the mutant.

The structures of the individual domains of the mutants are similar to their equivalents in the wild-type enzyme, with root-mean-square distances of 0.4–0.6 Å for C$\alpha$ atoms. The overall structure of the R54E mutant tetramer is also similar to that of the wild-type tetramer (Figure 3A). The second monomer of the mutant BC dimer shows an only 2° rotation relative to that of the wild-type dimer, after the first monomers of the two dimers are superimposed (Figure 3B). In the dimer interface, the side chain of Arg406 rearranges to interact with the new Glu54 side chain, while most of the other residues show only small changes (Figure 3C).


dx.doi.org/10.1021/bi301294d | *Biochemistry* 2013, 52, 488–496

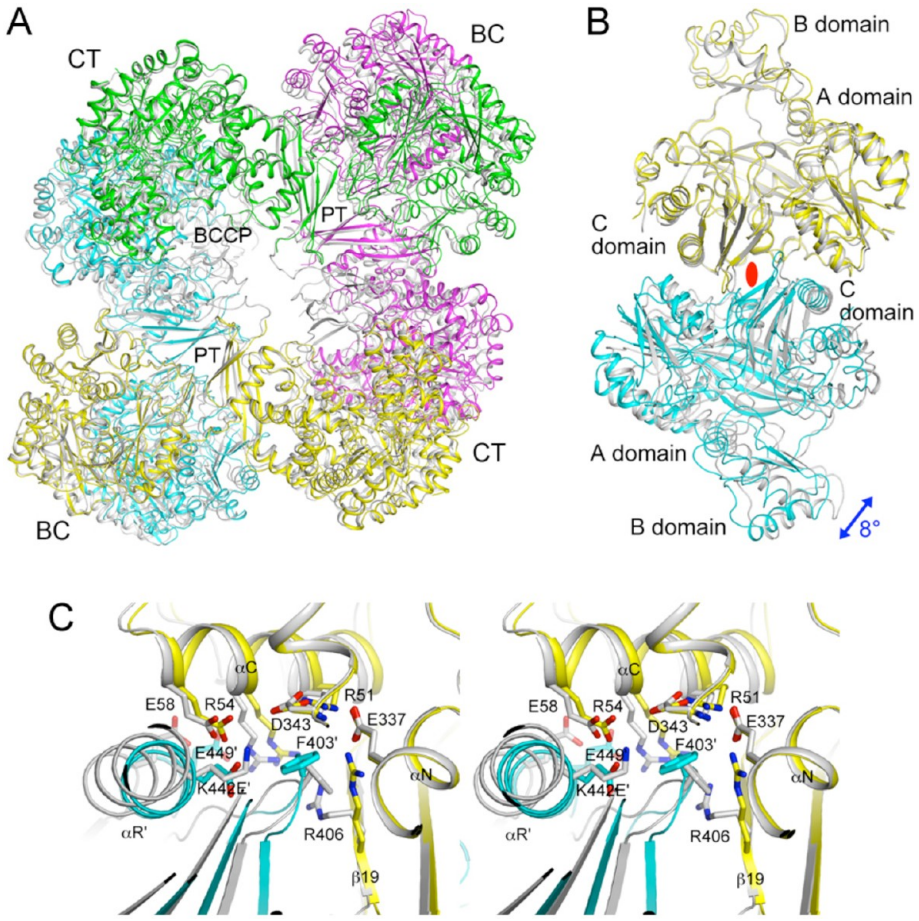


**Figure 5.** K442E mutant that is a tetramer in the crystal but shows large structural differences vs wild-type SaPC. (A) Overlay of the structures of the K442E mutant tetramer (in color) and wild-type SaPC (gray). The superposition is based on the BC domain of the first monomer (yellow). (B) Overlay of the structures of the K442E mutant BC domain dimer (yellow and cyan) and wild-type SaPC dimer (gray). (C) Close-up of the BC domain dimer interface near the mutation site.

In comparison, larger changes in the organization of the tetramer (Figure 4A) and dimer (Figure 4B) are observed for the F403A mutant, even though the mutation did not affect the $K_d$ of the tetramer (Table 2). A relative rotation of 4° is observed for the second monomer of the two dimers (Figure 4B). In the absence of the Phe403 side chain, the side chain of Arg406 undergoes a large conformational change, with its guanidinium group moving by ~5.5 Å (Figure 4C). The position of this side chain in the wild-type structure is no longer compatible with the dimer interface of the mutant as it clashes with the loop containing the mutation site (F403A). A change in the position of helix $\alpha$C is also observed (Figure 4C), possibly coupled with the reorganization of the dimer interface.

The K442E mutant also shows large changes in the organization of the tetramer (Figure 5A) and dimer (Figure 5B) as compared to wild-type SaPC. The rotation is 8° for the second monomer. Remarkably, the conformational changes in the dimer interface itself are rather similar to that observed for the F403A mutant (Figure 4F), although the structures of the two mutants differ from each other away from the interface.

**The Isolated BC Domain of SaPC Is Monomeric and Catalytically Inactive.** The tetramerization of PC involves the BC, CT, and PT domains. Mutations in the BC domain dimer interface that could be detrimental may be compensated by interactions at the CT and PT dimer interfaces. In fact, earlier studies with a human PC construct that lacked the BC domain altogether showed that it was still a tetramer.[25] Therefore, to study the effects of dimer interface mutations on isolated BC, we next expressed and purified the BC domain of wild-type SaPC alone, as well as the corresponding R54E, F403A, and K442E mutants. Despite having a dimer interface similar to that of *E. coli* BC, gel filtration experiments showed that the isolated BC domain of wild-type SaPC is monomeric in solution. This is confirmed by sedimentation velocity AUC experiments, which gave a $K_d$ of 48 $\mu$M for the dimer (Table 2). The R54E, F403A, and K442E mutants have roughly the same $K_d$ as the wild-type BC domain (Table 2). On the other hand, most of the isolated BC domain proteins have a significant amount of aggregation (Table 3), suggesting that this domain on its own may not be very stable. Possibly in agreement with this, extensive efforts to crystallize these proteins were unsuccessful.

To test whether the isolated BC domains have catalytic activity, we used a coupled-enzyme assay that monitored the hydrolysis of ATP.[9] The proteins were at a concentration of 0.4 $\mu$M, and 40 mM biotin was also included in the assay. No catalytic activity was observed with any of the proteins, including the wild-type isolated BC domain, under the condition tested. This indicates that the monomeric BC domain of SaPC is catalytically inactive, in contrast to observations with the monomeric mutants of the *E. coli* BC subunit.[19]


dx.doi.org/10.1021/bi301294d | *Biochemistry* 2013, 52, 488−496

These results for the isolated BC domain of SaPC are also in contrast with those found for the BC domain of other pyruvate carboxylases. The crystal structure of the BC subunit of *Aquifex aeolicus* PC showed a dimeric organization that is rather similar to that of *E. coli* BC.[38] On the other hand, the BC domain of *Geobacillus thermodenitrificans* PC showed a very different dimeric association in the crystal,[39] even though residues in the dimer interface are conserved in this protein (Figure 1B). This BC domain existed in a monomer−dimer equilibrium in solution and was able to catalyze the hydrolysis of ATP in the presence of biotin, likely in its monomeric form.[40] A chimera replacing the BC domain of *G. thermodenitrificans* PC with the BC subunit of *A. aeolicus* PC was also catalytically active.[41]

Our studies show that proper dimerization of the BC domain in the tetramer of PC is important for its catalytic activity. Mutations in this interface that disturb the dimer have a negative impact on activity. On the other hand, the R54E mutant is still a tetramer but is catalytically inactive. This appears to be consistent with a long-range communication between the dimer interface and the active site, although the mechanism of this communication is not known. A recent study of *E. coli* ACC showed that while the BC dimer interface mutants are active as a monomer in vitro, they are insufficient to rescue cells that are defective in BC.[42] This suggests that dimerization of the BC subunit is important for ACC activity in vivo; most likely, dimerization is important for the assembly of this ACC holoenzyme.

## AUTHOR INFORMATION


### Corresponding Author

*Phone: (212) 854-5203. Fax: (212) 865-8246. E-mail: ltong@columbia.edu.



### Funding

This research was supported in part by National Institutes of Health (NIH) Grant DK067238 to L.T. and by grants from the National Science Council, Taiwan (98-2320-B-010-026-MY3), and the National Health Research Institute, Taiwan (NHRI-EX101-9947SI), to C.-Y.C. L.P.C.Y. was also supported by an NIH training program in Cellular and Molecular Foundations of Biomedical Science (GM008798). P.H.C. was also supported by an NIH Medical Scientist Training Program (GM007367).


### Notes

The authors declare no competing financial interest.

## ACKNOWLEDGMENTS


We thank Christine Huang for help with the kinetic assays and Neil Whalen for setting up the X29A beamline at the National Synchrotron Light Source.


## REFERENCES


(1) Wakil, S. J., Stoops, J. K., and Joshi, V. C. (1983) Fatty acid synthesis and its regulation. *Annu. Rev. Biochem. 52*, 537−579.

(2) Cronan, J. E., Jr., and Waldrop, G. L. (2002) Multi-subunit acetyl-CoA carboxylases. *Prog. Lipid Res. 41*, 407−435.

(3) Tong, L. (2005) Acetyl-coenzyme A carboxylase: Crucial metabolic enzyme and attractive target for drug discovery. *Cell. Mol. Life Sci. 62*, 1784−1803.

(4) Jitrapakdee, S., St. Maurice, M., Rayment, I., Cleland, W. W., Wallace, J. C., and Attwood, P. V. (2008) Structure, mechanism and regulation of pyruvate carboxylase. *Biochem. J. 413*, 369−387.

(5) Tong, L. (2012) Structure and function of biotin-dependent carboxylases. *Cell. Mol. Life Sci.*, 10.1007/s00018-012-1096-0.

(6) Knowles, J. R. (1989) The mechanism of biotin-dependent enzymes. *Annu. Rev. Biochem. 58*, 195−221.

(7) Guchhait, R. B., Polakis, S. E., Dimroth, P., Stoll, E., Moss, J., and Lane, M. D. (1974) Acetyl coenzyme A carboxylase system from *Escherichia coli*. Purification and properties of the biotin carboxylase, carboxyltransferase, and carboxyl carrier protein components. *J. Biol. Chem. 249*, 6633−6645.

(8) Tipton, P. A., and Cleland, W. W. (1988) Catalytic mechanism of biotin carboxylase: Steady-state kinetic investigations. *Biochemistry 27*, 4317−4325.

(9) Blanchard, C. Z., Lee, Y. M., Frantom, P. A., and Waldrop, G. L. (1999) Mutations at four active site residues of biotin carboxylase abolish substrate-induced synergism by biotin. *Biochemistry 38*, 3393−3400.

(10) Sloane, V., Blanchard, C. Z., Guillot, F., and Waldrop, G. L. (2001) Site-directed mutagenesis of ATP binding residues of biotin carboxylase. *J. Biol. Chem. 276*, 24991−24996.

(11) Waldrop, G. L., Rayment, I., and Holden, H. M. (1994) Three-dimensional structure of the biotin carboxylase subunit of acetyl-CoA carboxylase. *Biochemistry 33*, 10249−10256.

(12) Thoden, J. B., Blanchard, C. Z., Holden, H. M., and Waldrop, G. L. (2000) Movement of the biotin carboxylase B-domain as a result of ATP binding. *J. Biol. Chem. 275*, 16183−16190.

(13) Mochalkin, I., Miller, J. R., Evdokimov, A., Lightle, S., Yan, C., Stover, C. K., and Waldrop, G. L. (2008) Structural evidence for substrate-induced synergism and half-sites reactivity in biotin carboxylase. *Protein Sci. 17*, 1706−1718.

(14) Chou, C.-Y., Yu, L. P. C., and Tong, L. (2009) Crystal structure of biotin carboxylase in complex with substrates and implications for its catalytic mechanism. *J. Biol. Chem. 284*, 11690−11697.

(15) Janiyani, K., Bordelon, T., Waldrop, G. L., and Cronan, J. E., Jr. (2001) Function of *Escherichia coli* biotin carboxylase requires catalytic activity of both subunits of the homodimer. *J. Biol. Chem. 276*, 29864−29870.

(16) de Queiroz, M. S., and Waldrop, G. L. (2007) Modeling and numerical simulation of biotin carboxylase kinetics: Implications for half-sites reactivity. *J. Theor. Biol. 246*, 167−175.

(17) Shen, Y., Volrath, S. L., Weatherly, S. C., Elich, T. D., and Tong, L. (2004) A mechanism for the potent inhibition of eukaryotic acetyl-coenzyme A carboxylase by soraphen A, a macrocyclic polyketide natural product. *Mol. Cell 16*, 881−891.

(18) Weatherly, S. C., Volrath, S. L., and Elich, T. D. (2004) Expression and characterization of recombinant fungal acetyl-CoA carboxylase and isolation of a soraphen-binding domain. *Biochem. J. 380*, 105−110.

(19) Shen, Y., Chou, C.-Y., Chang, G.-G., and Tong, L. (2006) Is dimerization required for the catalytic activity of bacterial biotin carboxylase? *Mol. Cell 22*, 807−818.

(20) Chou, C.-Y., and Tong, L. (2011) Structural and biochemical studies on the regulation of biotin carboxylase by substrate inhibition and dimerization. *J. Biol. Chem. 286*, 24417−24425.

(21) Huang, C. S., Sadre-Bazzaz, K., Shen, Y., Deng, B., Zhou, Z. H., and Tong, L. (2010) Crystal structure of the a6b6 holoenzyme of propionyl-coenzyme A carboxylase. *Nature 466*, 1001−1005.

(22) Huang, C. S., Ge, P., Zhou, Z. H., and Tong, L. (2012) An unanticipated architecture of the 750-kDa a6b6 holoenzyme of 3-methylcrotonyl-CoA carboxylase. *Nature 481*, 219−223.

(23) Fan, C., Chou, C.-Y., Tong, L., and Xiang, S. (2012) Crystal structure of urea carboxylase provides insights into the carboxyltransfer reaction. *J. Biol. Chem. 287*, 9389−9398.

(24) St. Maurice, M., Reinhardt, L., Surinya, K. H., Attwood, P. V., Wallace, J. C., Cleland, W. W., and Rayment, I. (2007) Domain architecture of pyruvate carboxylase, a biotin-dependent multifunctional enzyme. *Science 317*, 1076−1079.

(25) Xiang, S., and Tong, L. (2008) Crystal structures of human and *Staphylococcus aureus* pyruvate carboxylase and molecular insights into the carboxyltransfer reaction. *Nat. Struct. Mol. Biol. 15*, 295−302.

(26) Yu, L. P. C., Xiang, S., Lasso, G., Gil, D., Valle, M., and Tong, L. (2009) A symmetrical tetramer for *S. aureus* pyruvate carboxylase in complex with coenzyme A. *Structure 17*, 823−832.
(27) Lietzan, A. D., Menefee, A. L., Zeczycki, T. N., Kumar, S., Attwood, P. V., Wallace, J. C., Cleland, W. W., and St. Maurice, M. (2011) Interaction between the biotin carboxyl carrier domain and the biotin carboxylase domain in pyruvate carboxylase from *Rhizobium etli*. *Biochemistry 50*, 9708−9723.
(28) Schuck, P. (2003) On the analysis of protein self-association by sedimentation velocity analytical ultracentrifugation. *Anal. Biochem. 320*, 104−124.
(29) Brown, P. H., and Schuck, P. (2006) Macromolecular size-and-shape distributions by sedimentation velocity analytical ultracentrifugation. *Biophys. J. 90*, 4651−4661.
(30) Schuck, P. (2000) Size-distribution analysis of macromolecules by sedimentation velocity ultracentrifugation and Lamm equation modeling. *Biophys. J. 78*, 1606−1619.
(31) Modak, H. V., and Kelly, D. J. (1995) Acetyl-CoA-dependent pyruvate carboxylase from the photosynthetic bacterium *Rhodobacter capsulatus*: Rapid and efficient purification using dye-ligand affinity chromatography. *Microbiology 141*, 2619−2628.
(32) Otwinowski, Z., and Minor, W. (1997) Processing of X-ray diffraction data collected in oscillation mode. *Methods Enzymol. 276*, 307−326.
(33) Jogl, G., Tao, X., Xu, Y., and Tong, L. (2001) COMO: A program for combined molecular replacement. *Acta Crystallogr. D57*, 1127−1134.
(34) Brunger, A. T., Adams, P. D., Clore, G. M., DeLano, W. L., Gros, P., Grosse-Kunstleve, R. W., Jiang, J.-S., Kuszewski, J., Nilges, M., Pannu, N. S., Read, R. J., Rice, L. M., Simonson, T., and Warren, G. L. (1998) Crystallography & NMR System: A new software suite for macromolecular structure determination. *Acta Crystallogr. D54*, 905−921.
(35) Murshudov, G. N., Vagin, A. A., and Dodson, E. J. (1997) Refinement of macromolecular structures by the maximum-likelihood method. *Acta Crystallogr. D53*, 240−255.
(36) Jones, T. A., Zou, J. Y., Cowan, S. W., and Kjeldgaard, M. (1991) Improved methods for building protein models in electron density maps and the location of errors in these models. *Acta Crystallogr. A47*, 110−119.
(37) Emsley, P., and Cowtan, K. D. (2004) Coot: Model-building tools for molecular graphics. *Acta Crystallogr. D60*, 2126−2132.
(38) Kondo, S., Nakajima, Y., Sugio, S., Yong-Biao, J., Sueda, S., and Kondo, H. (2004) Structure of the biotin carboxylase subunit of pyruvate carboxylase from *Aquifex aeolicus* at 2.2 Å resolution. *Acta Crystallogr. D60*, 486−492.
(39) Kondo, S., Nakajima, Y., Sugio, S., Sueda, S., Islam, M. N., and Kondo, H. (2007) Structure of the biotin carboxylase domain of pyruvate carboxylase from *Bacillus thermodenitrificans*. *Acta Crystallogr. D63*, 885−890.
(40) Sueda, S., Islam, M. N., and Kondo, H. (2004) Protein engineering of pyruvate carboxylase. Investigation on the function of acetyl-CoA and the quaternary structure. *Eur. J. Biochem. 271*, 1391−1400.
(41) Islam, M. N., Sueda, S., and Kondo, H. (2005) Construction of new forms of pyruvate carboxylase to assess the allosteric regulation by acetyl-CoA. *Protein Eng. 18*, 71−78.
(42) Smith, A. C., and Cronan, J. E. (2012) Dimerization of the bacterial biotin carboxylase subunit is required for acetyl coenzyme A carboxylase activity in vivo. *J. Bacteriol. 194*, 72−78.